CellPress
REVIEWS

Opinion

Predicting Chronic Climate-Driven Disturbances and Their Mitigation

Nate G. McDowell,[1,*] Sean T. Michaletz,[2] Katrina E. Bennett,[2] Kurt C. Solander,[2] Chonggang Xu,[2] Reed M. Maxwell,[3] and Richard S. Middleton[2]

Society increasingly demands the stable provision of ecosystem resources to support our population. Resource risks from climate-driven disturbances, including drought, heat, insect outbreaks, and wildfire, are growing as a chronic state of disequilibrium results from increasing temperatures and a greater frequency of extreme events. This confluence of increased demand and risk may soon reach critical thresholds. We explain here why extreme chronic disequilibrium of ecosystem function is likely to increase dramatically across the globe, creating no-analog conditions that challenge adaptation. We also present novel mechanistic theory that combines models for disturbance mortality and metabolic scaling to link size-dependent plant mortality to changes in ecosystem stocks and fluxes. Efforts must anticipate and model chronic ecosystem disequilibrium to properly prepare for resilience planning.

Chronic Disturbances and Impacts on Ecosystem Services

The chronic rise in global temperature and temperature extremes [1,2] is resulting in an increase in climate-driven disturbances, such as wildfire and insect and pathogen outbreaks, that are unprecedented in recorded history [3]. Disturbances alter the ability of ecosystems to provide services essential to societal well-being [4]. Ecosystem services are inextricably linked with infrastructure in myriad ways, from the storage of carbon and regulation of climate at the global scale to the provision of food, water, and energy [4]. These relationships have evolved with human society over millennia and have become increasingly critical as human population growth and affluence have accelerated. Thus, a greater demand now exists for stable ecosystems to safeguard against failing infrastructure and resource loss [5–7]. This confluence of escalating disturbance risk and greater dependency on ecosystem services and disturbance-sensitive infrastructure could expose society to increasing recovery costs for repair of damaged infrastructure [8].

Growing awareness of societal risks posed by a changing climate has led to water crises and failure to mitigate climate change to be ranked in the *Global Risks Report* as two of the greatest risks to global society, and the two with the largest impact on society [9]. This awareness has spurred scientific gains into the projection of climate impacts, such as vegetation and hydrologic disturbances, and justifies the development of adaptation approaches to increase societal resilience to climate-driven hazards. However, the risks posed by climate-driven terrestrial disturbances remain underappreciated. Investment in mitigation and adaptation research (US $11.6 billion in the USA for 2013 [10]) is significantly less than the investment required to adapt to climate change (US$25 billion per year for 2010–2050 [11]) and by investment to combat

Trends

Terrestrial disturbances, such as wildfire, insect outbreaks, and drought-induced forest mortality, are increasing due to climate warming. Subsequent consequences for hydrological resources are simultaneously expanding.

The downstream impacts of the increasing frequency of disturbances are manifest as financial burden, loss of resource capacity, and impacts on human well-being. These threats of resource impacts due to chronic increases in disturbance frequency are now considered among the highest impact and highest likelihood of all threats to society.

Models of terrestrial disturbances and of hydrological resource responses to disturbances are rapidly improving, providing an opportunity for mitigation and adaptation planning.

Given current climate forecasts, it is likely that disturbance-induced threats to societally required resources will increase.

[1]Pacific Northwest National Laboratory, Richland, WA, USA
[2]Earth and Environmental Sciences Division, Los Alamos National Laboratory, Los Alamos, NM, USA
[3]Geology and Geological Engineering Department, Integrated Ground Water Modeling Center, Colorado School of Mines, Golden, CO, USA

*Correspondence: mcdowell@lanl.gov (N.G. McDowell).

traditional threats, such as terrorism (US$95 billion in the USA in 2013 [12]). Moreover, climate change exacerbates threats such as infectious diseases [13] and military conflicts [14].

The risk of a chronic decline in ecosystem services and the urgency to develop resiliency to climate-driven disturbances are at unprecedented levels. Fortunately, simulation advances within earth system models (ESMs; e.g., [15–18]) and climate downscaling tools [19] now enable high-resolution projection of impacts at regional scales (the scale at which impacts are felt), thereby enabling decision-making regarding adaptation and mitigation [20–23]. Thus, the opportunity, need, and potential exist to improve the resilience of societal infrastructure in the face of escalating disturbances [24,25]. However, to best capitalize on these capabilities, we must focus simulation and adaptation on the no-analog conditions that are being created by chronic disturbances. Here, we outline the concepts underlying a chronic decline in ecosystem services due to climate-driven disturbances (the chronic disequilibrium hypothesis) and discuss research opportunities that will enable improved ESM prediction of future disturbances. We focus on how drought and increasing temperatures influence water as a critical resource that both drives disturbances and responds to them, because these climatic drivers of disturbances are also expected to increase [4], although our framework could incorporate numerous other disturbances that are expected to increase in likelihood, such as floods and storms [4]. Likewise, we focus on literature from woody ecosystems, although our framework may be extensible to other ecosystems where the frequency of disturbance is expected to increase.

Climate-Driven Disturbances and the New State of Disequilibrium

Disturbances, such as drought, wildfire, and insect outbreaks, are climate driven because extremes in air temperature and precipitation drive their spatial magnitude and ultimate severity [26]. The mechanisms driving these disturbances vary regionally in relation to plant and insect species distributions, and historical management and disturbance regimens. However, the mechanisms by which warmer temperatures and droughts promote these disturbances are global. Dry periods, particularly those that occur under warm conditions, promote each of these disturbances [26] (although climate warming and drought may not always result in insect attacks [27]). This is alarming because, while forecasted precipitation is variable [28], air temperature increases are global and rising chronically [29], particularly over land surfaces [30].

Recent evidence is consistent with predicted increases in disturbance events. Forest mortality has doubled in North America and the Amazon basin [31,32] and predictions suggest greater mortality in the near future throughout the northern hemisphere [32,33]. Insect outbreaks and wildfires are now common in North America [3,34], and these disturbances have grown in frequency and extent throughout recent decades in Europe [35]. Human impacts upon reservoirs, water delivery, power generation, and crop production have increased dramatically in recent decades (see the supplemental information online for a brief review of these impacts).

Despite progress in global treaties to limit fossil fuel emissions[i], the committed warming is still likely to increase the frequency of climate-driven disturbances [4], potentially into a chronic state of disequilibrium (see description below). Due primarily to the projected warming increase, models consistently suggest widespread and severe increases in disturbances over the next century, particularly in regions where the provision of resources is already tenuous due to water limitations (e.g., [26,32,36]). The acceleration in disturbances is a result of the nonlinear dependence of the atmospheric vapor pressure deficit (VPD) on temperature (Figure 1A) [26,37,38], which causes vegetation stress (Figure 1B) by driving greater evaporation and, thus, greater degrees of hydraulic failure, carbon starvation, vulnerability to insects and pathogens [35], and fuel drying [39]. Consequently, chronic warming increases the likelihood that terrestrial ecosystems will succumb to periods of low precipitation via drought- and heat-induced mortality [40], insect- and pathogen-driven mortality [27], or wildfire [34].

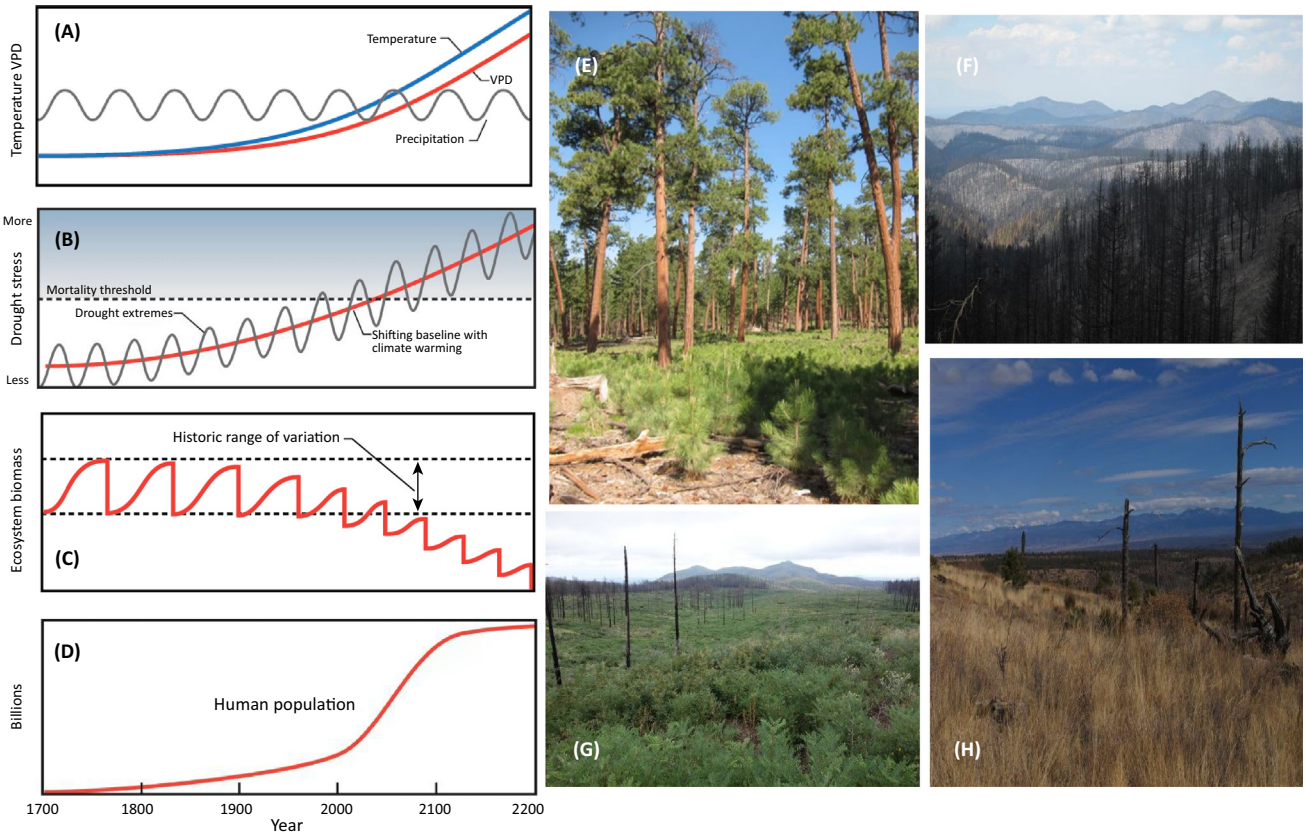

Trends in Ecology & Evolution

Figure 1. Figurative Representations of the Convergence of Increasing Temperature, Ecosystem Stress, Ecosystem Disequilibrium, and Human Population. (A) Increasing temperature results in an increasing vapor pressure deficit (VPD), which is overlain by the natural variation in precipitation over time. (B) The increasing VPD and variation in precipitation from (A) translate into an increasing drought stress baseline and more frequent and longer periods of drought stress that surpass the threshold for disturbance-induced mortality (gray line). (C) As more frequent and more severe disturbance events occur, the ecosystem biomass declines due to reduced time for recovery before a subsequent disturbance, resulting in chronic disequilibrium. (D) For reference, human population growth expectations over time show an increase simultaneous with increasing temperature and chronic ecosystem disturbance. Examples of the disequilibrium process, moving from (E) intact forest to (F) catastrophically burned forest to (G) shrubland and finally to (H) post-burned shrubland dominated by grassland.

The Chronic Disequilibrium Hypothesis

Future climate is expected to change until the average conditions exceed the severity of even the severest extremes in recorded history [26], with future extremes becoming more frequent, more severe, and of longer duration [7] (Figure 1C). A critical planning consideration from this evolving climate is the creation of chronic ecosystem disequilibrium (Figure 1C) that can force novel conditions beyond the historical range of variability [36,39]. Historically, a discrete, climate-driven disturbance would reduce ecosystem biomass and subsequent ecosystem functioning, but the extreme climate event that drove the disturbance (e.g., drought) would eventually dissipate and the system would recover [41,42]. Under current and future climate, the postdisturbance system will be subject to chronic warming, such that additional extreme events will become more likely to occur sooner and with more severity (Figure 1C) [43], precluding the system from reacquiring its prior structure and function [44] (although this is also a function of system growth rates post disturbance, which is influenced by CO_2 fertilization; reviewed in [3]). Each disturbance reduces stand biomass (Box 1) in part via size-dependent mortality (Box 2); thus the progressive increase in disturbance will accelerate biomass decline (and alter other ecosystem processes; Box 1) if recovery time is insufficient. A chronic disequilibrium ensues in which stable states are never reachieved, but instead a consistent

reduction in standing biomass and function repeats itself. This differs from a chaotic state because of the chronic trajectory that is maintained over extended periods [45].

Chronic disequilibrium has been observed in the paleorecord during particularly extended or higher-frequency, repeated climatic events that promoted the reorganization of vegetation composition (e.g., [46–52]). These reorganization events typically happened at regional scales, particularly after droughts occurred with anomalously high frequency over multiple decades (e.g., [39,48]). A recent example is the prolonged (multidecadal) and increasing water stress in *Pinus ponderosa* trees in New Mexico, which has resulted in regional losses and conversion to *Juniperus monosperma* woodlands from the 1950s to the present day [53,54] (C. Allen unpublished data, 2017).

The difference between historical periods of disequilibrium and today is twofold. First, previous periods of disequilibrium had inevitable stabilization because there was no outside forcing with a chronic trajectory similar to fossil fuel-derived increases in atmospheric CO_2 (e.g., [54]).

Box 1. Linking Size-Dependent Disturbance Mortality to Ecosystem Stocks and Fluxes

Current climate-change projections predict monotonic increases in air temperature and VPD (see Figure 1 in the main text) overlain with periods of low precipitation (see Figure 2 in the main text), which have the combined result of promoting more frequent and severe disturbances. Metabolic scaling theory (MST; Equations I–IV below) [60] show that these projections could lead to continued decreases in total ecosystem biomass, production, and transpiration. We develop here the theory for disturbance cause, size-dependent shifts in biomass, and fluxes for autotrophic (living) ecosystem components only, but metabolic scaling theory could also be developed for the heterotrophic ecosystem fluxes [61].

Plant mortality from climate-driven disturbances is generally size dependent [82,83]. Projected increases in disturbance frequency, duration, and severity (see Figure 1 in the main text) will alter the size distributions of disturbed areas. This will in turn influence ecosystem stocks and fluxes, such as biomass and production. Here, we outline MST that links stand size distributions to key autotrophic stocks and fluxes. In Box 2, we outline mechanistic theory for the alteration of stand size distributions by size-dependent fire and drought mortality. Together, these theories provide an approach for linking climate-driven disturbance mortality to ecosystem functioning from first principles.

Biomass is governed by the size distribution of the stand. MST for ecosystems shows that total autotrophic, ecosystem biomass M_{tot} (kg) can be quantified in terms of the stand size distribution [60], such that (Equation I):

$$M_{tot} = \frac{3}{5} c_n c_m^{-8/3} [r_{max}^{5/3} - r_{min}^{5/3}] = \frac{3}{5} c_n c_h^{-5/2} c_m^{-8/3} [h_{max}^{5/2} - h_{min}^{5/2}] \quad [I],$$

where c_n (m) is a size-corrected measure of the number of individuals of a given size, c_h ($m^{1/3}$) is a normalization constant relating stem height to stem radius, c_m (m $kg^{-3/8}$) is a normalization constant relating stem radius r (m) to plant mass, r_{min} (m) is the stem radius of the smallest individual, r_{max} (m) is the stem radius of the largest individual, h_{min} (m) is the height of the smallest individual, and h_{max} (m) is the height of the largest individual (see the supplemental information online for the full derivation of all equations). Equation I predicts that total biomass will increase as the 5/3 power of the stem radius and the 5/2 power of the height of the largest individual, and will decrease with the 5/3 power of the radius and the 5/2 power of the height of the smallest individual.

The theory can be further extended to ecosystem fluxes such as gross primary production, net primary production, and canopy transpiration. Specifically, the total gross primary production rate GPP_{tot} (kg yr^{-1}) can be expressed as (Equation II) [60]:

$$GPP_{tot} = GPP \cdot A = g_0 c_n [r_{max} - r_{min}] = g_0 c_n c_h^{-3/2} [h_{max}^{3/2} - h_{min}^{3/2}] \quad [II],$$

where GPP (kg m^{-2} yr^{-1}) is gross primary production, A (m^2) is the stand area under consideration, and g_0 (kg m^{-2} yr^{-1}) is a gross production normalization constant. Similarly, the total net primary production rate NPP_{tot} (kg yr^{-1}) can be characterized as (Equation III) [81]:

$$NPP_{tot} = NPP \cdot A = n_0 c_n [r_{max} - r_{min}] = n_0 c_n c_h^{-3/2} [h_{max}^{3/2} - h_{min}^{3/2}] \quad [III],$$

where NPP (kg m^{-2} yr^{-1}) is net primary production and n_0 (kg m^{-2} yr^{-1}) is a net production normalization constant. Finally, the total canopy transpiration rate E_{tot} (kg yr^{-1}) is given by Equation IV

$$E_{tot} = E \cdot A = \alpha^{-1} n_0 c_n [r_{max} - r_{min}] = \alpha^{-1} n_0 c_n c_h^{-3/2} [h_{max}^{3/2} - h_{min}^{3/2}] \quad [IV],$$

where α (kg kg^{-1}) is the water-use efficiency of production. Thus, Equations II–IV predict that rates of ecosystem production and transpiration will scale isometrically with stem radius and the 3/2 power of plant height, increasing with the radius and height of the largest individual and decreasing with the radius and height of the smallest individual.

These formulations are further developed within the supplemental information online.

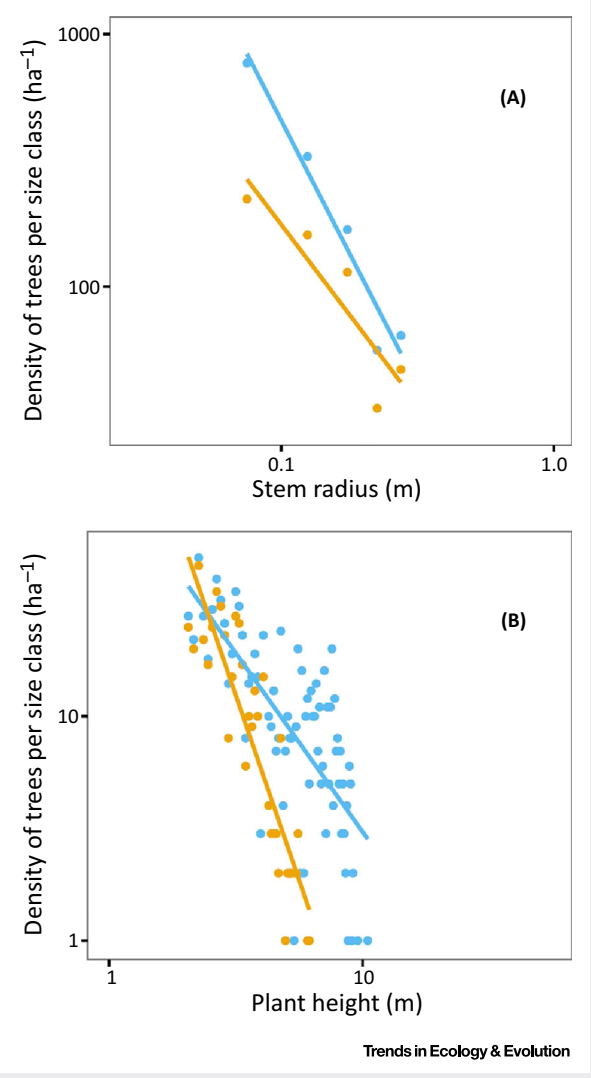

Figure I. Effects of Size-Dependent Disturbance Mortality on Forest Size Distributions. (A) Relationship between density of trees per size class and stem radius at breast height for a tropical forest in Malaysia before (blue) and after (orange) a fire. Data points were calculated from empirical data in [79]. The reduced major axis (RMA) regression slope before the fire was −2.15 (95% CI = −3.20 to −1.45), which does not differ from the metabolic scaling theory (MST) prediction of −2. The RMA regression slope after the fire was −1.58 (95% CI = −3.28 to −0.76), which reflects size-dependent fire mortality of the smallest size classes. (B) Relationship between density of trees per size class and plant height for a piñon-juniper woodland before (blue) and during (orange) a drought. Data points were calculated from empirical data in [80]. The Pareto MLE slope before the drought was −2.43 (95% CI = −2.52 to −2.34). This slope is greater than the MST prediction of −3, which reflects the effects of an earlier drought at this site [80]. The Pareto MLE slope after the drought was −3.69 (95% CI = −3.94 to −3.44), which reflects size-dependent drought mortality of the largest size classes.

Box 2. Examples of Size-Dependent Mortality from Wildfire and Drought-Induced Mortality

Ecosystem stocks and fluxes are strongly influenced by size-dependent disturbance mortality because they are governed by the size distribution of the plant stand (Box 1). Here, we consider two examples of disturbance mortality (fire and drought/insect attack), but the same theory applies to other climate-driven disturbances, such as floods and pathogen outbreaks. These formulations are further developed within the supplemental information online.

Fire mortality is nearly always size dependent and kills the smaller size classes before the larger size classes [82]. This applies to all fires, from low-intensity surface fires (such as those that dominate Eurasia) to high-intensity crown fires (such as those that have become common in North America) [59], although the size of killed trees will generally increase with intensity [82]. It is rare, even for stand-replacing fires, to kill all trees. If fire frequencies increase, there will be progressively fewer small trees to grow into larger size classes, and subsequently, based on Equation I in Box 1, a progression of decreased biomass is likely. Fire-induced mortality results from interactions of multiple injuries to tissues in the plant roots, stem, and crown [84]. For illustration purposes, we consider a single fire mortality mechanism (vascular cambium necrosis). Process-based models show that the radius of the smallest stem that will survive fire is (Equation I) [82]:

$$r_{min} = \frac{x_n - b}{2a} \quad [I],$$

where x_n is the depth of tissue necrosis in the stem (m) and a and b are fitted coefficients from linear cambial depth allometries (see the supplemental information online for more-detailed derivations). The depth of tissue necrosis is given by an analytical solution for Fourier's law of conduction (Equation II) [82]:

$$x_n = 2[\alpha\ t]^{1/2}\ \ erf^{-1}\left(\frac{60 - T_f}{T_a - T_f}\right) \quad [II],$$

where α is the thermal diffusivity of bark ($m^2\ s^{-1}$), t is the fire residence time (s), T_f is the fire temperature (°C), and T_a is the air temperature (°C). The fire temperature T_f (°C) scales with air temperature and fireline intensity I (kW m^{-1}) [82], such that (Equation III):

$$T_f \propto T_a^{1/3} I^{2/3} + T_a \quad [III],$$

Thus, Equations I–III show how fire mortality, via r_{min}, can alter the size distribution of a plant stand. Fire mortality is under direct climatic control, given the role of air temperature and VPD in fuel drying, fireline intensity, and fire spread. Figure IA shows data from a tropical forest in Malaysia before and after a forest fire [79]. By preferentially killing the smallest size classes, this fire reduced the slope of the size-frequency distribution from −2.15 (95% CI = −3.20 to −1.45), which agrees with the MST prediction of −2, to −1.58 (95% CI = −3.28 to −0.76). Note that these slopes are predictable from the initial size distribution and Equations I–III when plant trait and fire behavior data are available. Two important notes relate to this example: (i) fires lead to reduced biomass; and (ii) increases in fire frequency will limit the recruitment of small size classes that could grow into large size classes, such that attrition of large size classes over time will ultimately lead to reductions in ecosystem stocks and fluxes.

Drought- and insect-associated mortality are also size dependent, and generally kill the largest trees [83], which provide the greatest benefits to the ecosystem (carbon storage, water use, and wildlife habitat). Drought mortality occurs when the available supply of water to a plant cannot meet the evaporative demand for water from the plant [38], followed by insect attack in many cases. This can be characterized using the hydraulic corollary of Darcy's Law (Equation IV) [38]:

$$h_{\max} = \frac{A_s k_s [\psi_s - \psi_l]}{G \eta A_l VPD} \quad [IV],$$

where G is the canopy-scale water conductance (mol $m^{-2}\ s^{-1}$), h_{max} is the maximum plant height that can be hydraulically supported (m), A_s is the conducting area (cm^2), A_l is the leaf area (m^2), k_s is the specific conductivity (m s^{-1}), η is the water viscosity (Pa s), $\psi_s - \psi_l$ is the soil-to-leaf water potential difference (MPa) and VPD is the vapor pressure deficit (kPa). Increasing temperature (with assumed increasing absolute humidity [37]) and decreasing relative humidity during drought force increases in VPD, and, all else being equal, a reduction in the maximum plant height that can be hydraulically sustained [38]. Drought-driven reductions in maximum plant size can have large impacts on the size distribution of disturbed areas. For example, Figure IB shows size-frequency distributions for a woodland in New Mexico before and during a drought [80]. By preferentially killing the largest size classes, this drought reduced the slope of the size-frequency distribution from −2.43 (95% CI = −2.52 to −2.34) to −3.69 (95% CI = −3.94 to −3.44). Again, these slopes are also predictable from the initial size distribution and Equation IV, provided plant trait and drought data are available.

Current climate-change projections predict monotonic increases in air temperature and VPD (see Figure 1 in the main text) coupled with continued periodicity of low precipitation (see Figure 2 in the main text). Thus, all being else equal, Equations I–IV in Box 1 and I–III here show that projected increases in these climate variables could lead to continued decreases in total ecosystem biomass production and transpiration. Although we have not discussed decomposition carbon fluxes here, they are influenced by the input of necromass post disturbance, leading to further dynamics in net ecosystem carbon storage [61].

Second, the rates of environmental change expected in upcoming decades exceed those recorded in history [54]; thus, the possibility exists that chronic ecosystem disequilibrium in the future will be more rapid and severe than that observed in the paleorecord.

Compensating ecological processes, such as increasing terrestrial photosynthesis, may slow the loss of ecosystem function resulting from chronic disturbances, but these offsets are expected to be outweighed by the chronic 'push' of temperature increase (both means and extremes) due to the slow nature of most compensating responses relative to the rate of climate warming [4]. Increasingly, we have observations of the changing vegetation composition of ecosystems, such that they become entirely new systems (Figure 1E–H; [55]). These system changes are akin to 'phase changes' in physics, where intrinsic properties are altered, such as the structure of the vegetation, and associated biogeochemical and energetic fluxes between the ecosystem and surrounding environment. Even if the system maintains the same vegetation but the plant size distribution is altered, the increased frequency of disturbances may prevent the vegetation from achieving a resource and demographic steady state, forcing a chronic trajectory of the system towards nonoptimal space filling with less carbon storage and flux (Figure 1C and Box 1) [38], greater erosion, and altered hydrology. Chronic ecosystem disequilibrium is driven in part by the growing likelihood of ecosystems reaching their tipping points [56,57], because the system is more apt to cross thresholds into new ecological regimens. Understanding how chronic disturbances and associated tipping points will impact ecosystem services is a critical link to providing mitigation solutions under climate warming [58].

Scaling Individual Plant Mortality to Ecosystem Stocks and Fluxes

Plant mortality from climate-driven disturbances is nearly always size dependent (Box 2) [82,83] and, thus, alters the size distribution of plants within the disturbed area. Alterations in the stand size distribution will in turn influence autotrophic stocks and fluxes, such as biomass, production, and transpiration. Extension of metabolic scaling theory (MST) [60] allows linkage of size-dependent disturbance mortality to autotrophic stocks and fluxes (Box 1). Biomass and fluxes scale with the stand distributions of stem radius and total plant height (Box 1), two variables that are mechanistically influenced by climate-driven mortality. Based on this relatively well-tested theory [60], chronically increasing disturbance rates will cause ecosystem biomass, production, and transpiration to decline (consistent with [52]). These first-principle formulations are testable using empirical data, and allow the extension of structural impacts to predict functional impacts of disturbance, and may facilitate ESM development (see below). In Box 2, we outline mechanistic zeroth-order theories for size-dependent mortality from two types of climate-driven disturbance: wildfire and drought. We consider these two examples for simplicity, but the same general theory applies to other climate-driven disturbances, such as floods or pathogen outbreaks. Ultimately, the strong dependence of fluxes upon biomass (Box 1) coupled to a progressively decreasing biomass will result in decreasing overall fluxes, such as carbon uptake (a dominant climate regulator), primary production (critical for crop and wood yield), or water consumption (influencing local hydrology).

Scaling theory presented in Box 1 can also be applied to understand the recovery of autotrophic biomass and function post disturbance if plant size-class distributions are known. If biomass increases more rapidly post disturbance under higher CO_2 (reviewed in [4]), then we can expect the post-disturbance biomass and fluxes to reachieve predisturbance values at a faster rate based on the theory in Box 1 and associated information in the supplemental information online. The obvious question this poses is, which is faster: the rate of increase in severe disturbances, or the rate of recovery post disturbance? The answer will dictate whether chronic ecosystem disequilibrium manifests (e.g., Figure 1C,D). Empirical and modeling evidence thus far suggests increasing disturbances in the 21st century may overwhelm increasing growth and cause a reduction in ecosystem biomass [4,32,33]. Notably, decomposition fluxes

will be influenced by disturbances [61]; thus, total ecosystem carbon balance will be the net result of both auto- and heterotrophic carbon fluxes.

What Regions Will Be Most Vulnerable to Climate Change-Driven Disturbances in the Future?

It is naïve to assume that only drier regions will experience drought- and heat-induced mortality events. A higher capacity for energy, carbohydrate, and water storage in wetter systems provides a greater buffer against drought impacts (e.g., see [62] for an example across an elevation gradient). However, the negative impacts of increasing VPD are greatest in wetter systems due to their higher stomatal sensitivity to VPD [38,63]. We assessed Coupled Model Intercomparison Project [16] model predictions of drought likelihood as defined by the 20-cm soil moisture below its second percentile from 1850 to 2100 across the Earth under climate warming (Figure 2). We found that the area of the Earth exposed to severe drought will increase over the next 80 years, due primarily to the influence of increasing temperature on evaporation (Figure 2A,B). Although regions of relatively low precipitation experience the greatest increase in drought likelihood, even wet systems are likely to experience a doubling of drought frequency by 2100 (Figure 2C,D), due primarily to warming and greater evaporative water loss. This is consistent with predictions that all locations experience drought, but, as the future becomes warmer, the resilience associated with mesic systems will decline as the frequency and severity of droughts increases [4,38]. Thus, risks of climate-driven disturbances will increase even in areas that historically had limited drought disturbances. Given that no region is immune from increasing climate-driven disturbances, our focus must be on global-scale mitigation and adaptation strategies [44].

The Future of Climate-Driven Disturbance Modeling

There are no clear analogs to the state of disequilibrium that we are entering (Figure 1) due to the rate of change and the near-chronic growth of the external forcing agent (industrial CO_2 [47,52,64]). The unique challenges of climate change include temperature increases, variable precipitation change, extreme climate events, and the larger, more severe, chronically increasing disturbances that create no-analog conditions (Figure 1). Few existing ESMs have considered chronic disequilibrium from climate-driven disturbances, in part because there are few historic observations appropriate for modeling a chronically warming future [20,54,64]. Consequently, this is both a challenge and opportunity for ESM-disturbance studies, in particular models that can mechanistically represent the processes driving future changes.

The state of computational modeling of climate-driven disturbances has improved dramatically over the past decade, but shortcomings remain. Downscaling ESMs to accurately capture the observed historical climate and extreme events remains one of our largest challenges [65]. Representations of forest mortality from drought and heat have improved from relatively non-mechanistic approximations of vegetation loss [40] to detailed, highly validated predictions [32,33,66]. Wildfire predictions remain challenged by an inability to predict ignition and spread mechanisms [67], although ESM-based wildfire models are becoming more mechanistic [68]. Predictions of pathogen and insect impacts are largely empirical and have not yet been incorporated into ESMs [69]. Simulations of climate feedbacks from disturbances have evolved in parallel with simulations of disturbance and are now being validated for energy and albedo shifts in ESMs [70]. Simulations of hydrologic impacts from disturbance utilize advanced hydrological and climatic models to simulate the streamflow and runoff responses from an artificially imposed disturbance [71–77]. Ultimately, these simulations must feed information to infrastructure-planning models that are being developed simultaneously (not covered here; see [4]). We do note that the greatest challenges infrastructure models may face beyond downscaling of driver data (e.g., climate) to appropriate resolutions, will be anticipating the failure of

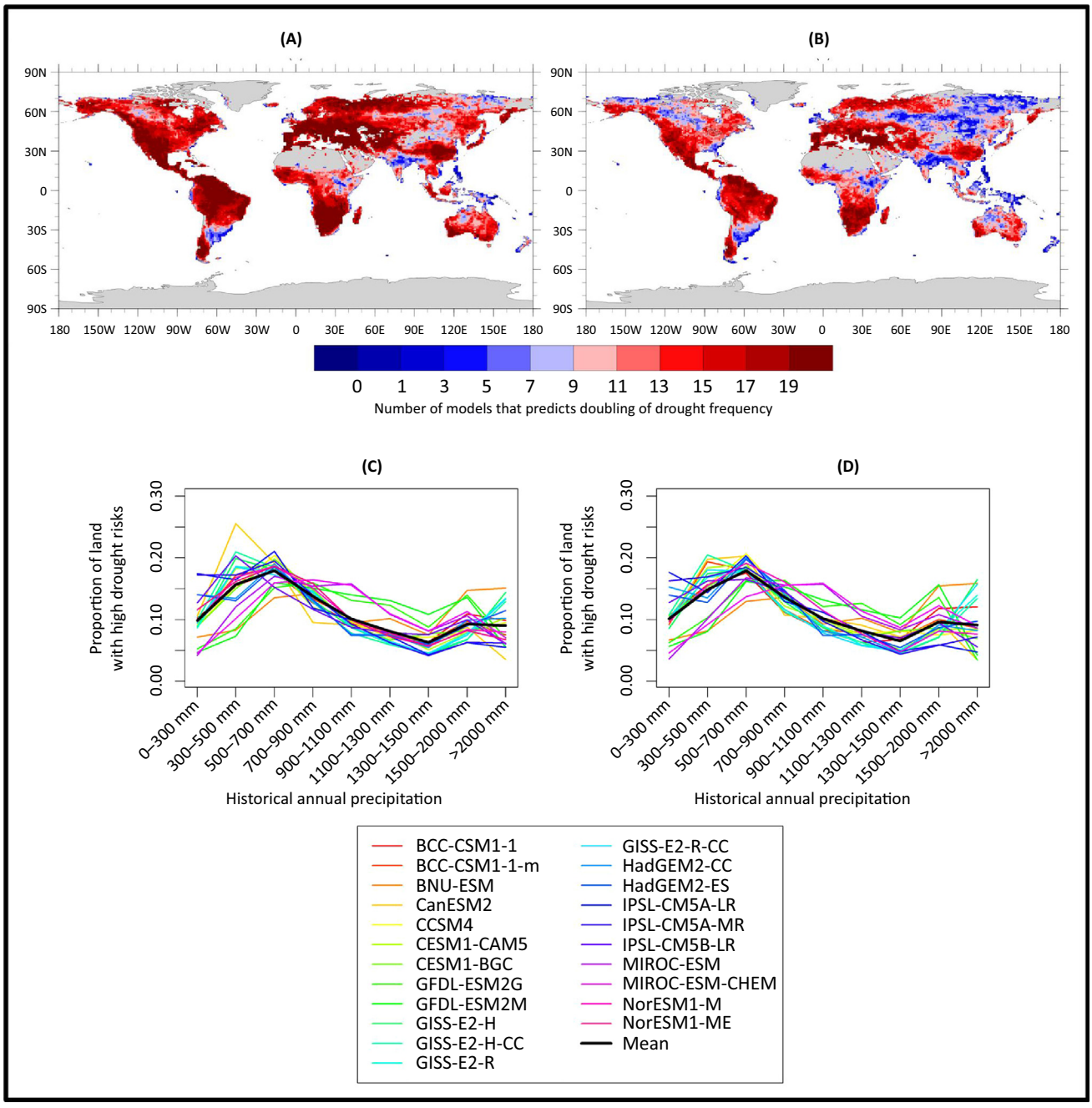

Trends in Ecology & Evolution

Figure 2. (A,B) The Fraction of Global Land Area that will be Exposed to Severe Droughts by 2100. Results from 22 models involved in the Coupled Model Intercomparison Project version 5 that show severe drought likelihood (defined as soil moisture in the top 10 cm that is below the 10th percentile of historical values for each grid cell) between 2000 and 2100. (A) Results using climate forcing from RCP 8.5 (business as usual fossil fuel emissions). (B) Climate forcing from RCP 4.5 (moderate limitations to fossil fuel emissions). (C,D) The fraction of global land area that will be exposed to severe droughts [from (A,B)] versus the historical average mean annual precipitation of all of the land falling within each drought category. From this figure, we can see that, as the climate warms, drought risk spreads into increasingly wet locations, highlighting that, in the future, few landscapes will be immune from climate-driven disturbances. Predictions for moderate and mild droughts are shown in the appendix.

ecosystem services to recover fully before subsequent disturbances (i.e., chronic disequilibrium).

Key modeling tasks to simulate disequilibrium impacts under increasing spatial and temporal threats of climate-driven disturbance must focus in part on the inability of ecosystems to recover to predisturbance conditions. For example, following a stand-replacing wildfire that alters regeneration trajectories, climate and hydrological feedbacks may not recover (Figure 1), thereby requiring mitigation and adaptation planning that allows for long-term and unique changes in ecosystem services, such as water provision [34,78]. In addition, model simulations must account for the increasing frequency of extreme events, such that ecosystem resources can be simulated to experience the risk of chronic disequilibrium. In the case of hydrology, the simulations should include improved representation of both ground water and transpiration [23] as well as changes in surface erosion, because sedimentation will increase in response to chronic disturbances causing long-term changes in the surface structure and in water quality. The partial recovery of terrestrial vegetation after disturbances [7] must also be considered because it may buffer erosion and other impacts. For management applications, the ability to downscale simulations to regional or local applications is a large challenge.

A pressing need is to first identify and characterize areas that are likely vulnerable to future climate-driven disturbances (as shown in Figure 2 at the global scale), and to understand how these vulnerable areas will impact critical ecosystem services. This will require next-generation mechanistic models of future ecosystems that can account for novel conditions and processes without relying on parameterizations based only on past behavior. For example, forest restoration projects could focus on replacing disturbed ecosystems with species that are resilient to future climate conditions, including increased temperature, drought, and extreme precipitation, as well as climate-driven disturbances. Under a warming climate, restoring forests with present-day species could lead to future mortality. Thus, a predictive science-based approach to disturbance would suggest climate-aware restoration, whereby species (and varieties) are identified that could be expected to survive warmer heat waves and droughts [34]. Similar modeling of adaptation to prolonged and repeated disturbances can be applied to infrastructure resilience (e.g., power production and irrigation).

Metabolic scaling theory (Boxes 1 and 2) can be useful within the goal of ESM predictions of changes in structure and function. Demographic ESMs (e.g., [15,18]) can predict size distributions of trees as well as fluxes, but require extensive parameterization and evaluation data sets. Using inventory or remotely sensed data of biomass as a driver, fluxes of carbon and water predicted by scaling theory and from the more physiologically mechanistic ESMs can be compared for independent evaluation. For reduced computational costs, coarse-resolution global ESM simulations can be run to predict size-dependent mortality and resulting stand size-frequency distributions, which can in turn be coupled to scaling theory to predict their impacts on ecosystem stocks and fluxes. This latter application can also be used at the local scale via inventory data or remote-sensing imagery to provide a practical tool for land managers to assess future impacts on fluxes of concern.

Concluding Remarks

The chronic increase in average and extreme temperatures is causing a chronic increase in climate-driven disturbances. This can drive ecosystems to enter a state of disequilibrium in which recovery to predisturbance states becomes less likely, causing not only many impacts, but also more questions (see Outstanding Questions). The impacts on ecosystem services will increase simultaneous with our increasing demand for ecosystem services, such as food, fuel, and water, due to a burgeoning global population. This confluence of risk and demand justifies immediate investment in the improved prediction of chronic disturbance impacts. Our

Outstanding Questions

What is the rate of decline in ecosystem services in response to chronically increasing climatic-disturbance drivers, and what is the rate and magnitude of recovery from disturbances given the chronic increase in CO_2?

What is the regional and local variation in chronic disturbances and associated impacts on resources such as water? What controls such variation?

Metabolic scaling theory predictions of decreasing ecosystem function under chronic disequilibrium must be tested rigorously; this will support fundamental understanding and improve future ESM simulations.

community should consider the long-term changes in ecosystem function driven by chronic warming in the context of chronic disturbance disequilibrium.

Author Contributions

N.G.M. and R.S.M. conceived of the manuscript content. All authors contributed to the writing. C.X. contributed the analyses for Figure 2 and S.M. contributed the theory and analyses for Boxes 1 and 2.

Acknowledgments

Craig Allen and three anonymous referees provided valuable critiques and edits to this manuscript. N.G.M. and R.S.M. conceived of the manuscript content. All authors contributed to the writing. C.X. contributed the analyses for Figure 2 and S.M. contributed the analysis for Box 2. N.G.M., K.B., S.M., K.S., C.X., and R.S.M. acknowledge the support of Los Alamos National Laboratories LDRD program. N.G.M. and C.X. acknowledge the support of Department of Energy, Office of Science. N.G.M. acknowledges the support of Pacific Northwest National Laboratories LDRD program. R.M.M. acknowledges the support of the National Science Foundation grant WSC-1204787.

Resources

[i]www.cop21paris.org/about/cop21www.cop21paris.org/about/cop21

Supplemental Information

Supplemental information associated with this article can be found, in the online version, at https://doi.org/10.1016/j.tree.2017.10.002.

References

1. IPCC (2013) *Climate Change 2013: The Physical Science Basis. Contribution of Working Group I to the Fifth Assessment Report of the Intergovernmental Panel on Climate Change,* Cambridge University Press
2. Seneviratne, S.I. *et al.* (2014) No pause in the increase of hot temperature extremes. *Nat. Clim. Change* 4, 161–163
3. Allen, C.D. *et al.* (2015) On underestimation of global vulnerability to tree mortality and forest die-off from hotter drought in the Anthropocene. *Ecosphere* 6, 1–55
4. IPCC (2014) *Climate Change 2014: Impacts, Adaptation, and Vulnerability. Part A: Global and Sectoral Aspects. Contribution of Working Group II to the Fifth Assessment Report of the Intergovernmental Panel on Climate Change,* Cambridge University Press
5. Barnosky, A.D. *et al.* (2012) Approaching a state shift in Earth's biosphere. *Nature* 486, 52–58
6. Gauthier, S. *et al.* (2015) Boreal forest health and global change. *Science* 349, 819–822
7. Millar, C.I. and Stephenson, N.L. (2015) Temperate forest health in an emerging era of megadisturbance. *Science* 349, 823–826
8. Changnon, S.A. (2006) *Railroads and Weather,* American Meteorological Society
9. World Economic Forum (2016) *The Global Risks Report 2016.* (11th edn), World Economic Forum
10. Leggett, J.A. *et al.* (2013) *Federal Climate Change Funding from FY2008 to FY2014,* Congressional Research Service
11. Backus, G.A. *et al.* (2012) The near-term risk of climate uncertainty among the U.S. states. *Clim. Change* 116, 495–522
12. Belasco, A. (2014) *The Cost of Iraq, Afghanistan, and Other Global War on Terror Operations Since 9/11,* Congressional Research Service
13. Altizer, S. *et al.* (2013) Climate change and infectious diseases: from evidence to a predictve framework. *Science* 341, 514–519
14. Gleick, P. (2014) Water, drought, climate change, and conflict in Syria. *Water Clim. Soc.* Published online July 1, 2014. http://dx.doi.org/10.1175/WCAS-D-13-00059.1
15. Moorcroft, P.R. *et al.* (2001) A method for scaling vegetation dynamics: the ecosystem demography model (ED). *Ecol. Monogr.* 71, 557–586
16. Taylor, K.E. *et al.* (2012) An overview of CMIP5 and the experiment design. *Bull. Am. Meteorol. Soc.* 93, 485–498
17. McDowell, N.G. *et al.* (2013) Evaluating theories of drought-induced vegetation mortality using a multi-model-experiment framework. *New Phytol.* 200, 304–321
18. Fisher, R.A. *et al.* (2015) Taking off the training wheels: the properties of a dynamic vegetation model without climate envelopes. *Geosci. Model Dev.* 8, 3293–3357
19. Pierce, D.W. *et al.* (2014) Statistical downscaling using localized constructed analogs (LOCA). *J. Hydrometeorol.* 15, 2558–2585
20. Bearup, L.A. *et al.* (2014) Hydrological effects of forest transpiration loss in bark beetle-impacted watersheds. *Nat. Clim. Change* 4, 481–486
21. Gould, G.K. *et al.* (2016) The effects of climate change and extreme wildfire events on runoff erosion over a mountain watershed. *J. Hydrol.* 536, 74–91
22. Hyde, K.D. *et al.* (2016) Influences of vegetation disturbance on hydrogeomorphic response following wildfire. *Hydrol. Process.* 30, 1131–1148
23. Maxwell, R.M. and Condon, L.E. (2016) Connections between groundwater flow and transpiration partitioning. *Science* 353, 377–380
24. Millar, C.I. *et al.* (2007) Climate change and forests of the future: managing in the face of uncertainty. *Ecol. Appl.* 17, 2145–2151
25. Leichenko, R. (2011) Climate change and urban resilience. *Curr. Opin. Environ. Sustain.* 3, 164–168
26. Williams, A.P. *et al.* (2013) Temperature as a potent driver of regional forest drought stress and tree mortality. *Nat. Clim. Change* 3, 292–297
27. Hicke, J.A. *et al.* (2006) Changing temperatures influence suitability for modeled mountain pine beetle (Dendroctonus ponderosae) outbreaks in the western United States. *J. Geophys. Res. Biogeosci.* 111
28. Trenberth, K.E. (2011) Changes in precipitation with climate change. *Clim. Res.* 47, 123–138
29. Hartmann, D.L. *et al.* (2013) Observations: atmosphere and surface. In *Climate Change 2013: The Physical Science Basis. Contribution of Working Group I to the Fifth Assessment Report of the Intergovernmental Panel on Climate Change* (Stocker, T.F., Qin, D., Plattner, G.-K., Tignor, M., Allen, S.K., Boschung, J., Nauels, A., Xia, Y., Bex, V. and Midgley, P.M., eds), Cambridge University Press
30. Boer, G.J. (2011) The ratio of land to ocean temperature change under global warming. *Clim. Dyn.* 37, 2253–2270
31. Brienen, R.J. *et al.* (2015) Long-term decline of the Amazon carbon sink. *Nature* 519, 344–348
32. McDowell, N.G. *et al.* (2016) Multi-scale predictions of massive conifer mortality due to chronic temperature rise. *Nat. Clim. Change* 6, 295–300

33. Anderegg, W.R. *et al.* (2015) Tree mortality predicted from drought-induced vascular damage. *Nat. Geosci.* 8, 367–371
34. Van der Werf, G.R. *et al.* (2010) Global fire emissions and the contribution of deforestation, savanna, forest, agricultural, and peat fires (1997–2009). *Atmos. Chem. Phys.* 10, 11707–11735
35. Seidl, R. *et al.* (2014) Increasing forest disturbances in Europe and their impact on carbon storage. *Nat. Clim. Change* 4, 806–810
36. Westerling, A.L. *et al.* (2011) Continued warming could transform Greater Yellowstone fire regimes by mid-21st century. *Proc. Natl. Acad. Sci. U. S. A.* 108, 13165–13170
37. Trenberth, K.E. *et al.* (2014) Global warming and changes in drought. *Nat. Clim. Change* 4, 17–22
38. McDowell, N. and Allen, C. (2015) Darcy's law predicts widespread forest loss due to climate warming. *Nat. Clim. Change* 5, 669–672
39. Swetnam, T.W. and Betancourt, J.L. (1990) Fire-southern oscillation relations in the southwestern United States. *Science (Washington)* 249, 1017–1020
40. McDowell, N.G. *et al.* (2011) The interdependence of mechanisms underlying climate-driven vegetation mortality. *Trends Ecol. Evol.* 26, 523–532
41. Odum, E.P. (1969) The strategy of ecosystem development. *Science* 164, 262–270
42. Odum, E.P. (1985) Trends expected in stressed ecosystems. *Bioscience* 35, 419–422
43. Adams, H.D. *et al.* (2009) Temperature sensitivity of drought-induced tree mortality portends increased regional die-off under global-change-type drought. *Proc. Natl. Acad. Sci. U. S. A.* 106, 7063–7066
44. Lenton, T.M. and Ciscar, J.C. (2013) Integrating tipping points into climate impact assessments. *Clim. Change* 117, 585–597
45. Tsonis, A.A. (2012) *Chaos: from theory to applications,* Springer Science & Business Media
46. Delcourt, H.R. *et al.* (1982) Dynamic plant ecology: the spectrum of vegetational change in space and time. *Quat. Sci. Rev.* 1, 153–175
47. Jackson, S.T. and Overpeck, J.T. (2000) Responses of plant populations and communities to environmental changes of the late Quaternary. *Paleobiology* 26 (sp4), 94–220
48. Gray, S.T. *et al.* (2006) Role of multidecadal climate variability in a range extension of pinyon pine. *Ecology* 87, 1124–1130
49. Fawcett, P.J. *et al.* (2011) Extended megadroughts in the southwestern United States during Pleistocene interglacials. *Nature* 470, 518–521
50. Booth, R.K. *et al.* (2012) Multi-decadal drought and amplified moisture variability drove rapid forest community change in a humid region. *Ecology* 93, 219–226
51. McLauchlan, K.K. *et al.* (2014) Reconstructing disturbances and their biogeochemical consequences over multiple timescales. *Bioscience* 64, 105–116
52. Jackson, S.T. and Blois, J.L. (2015) Community ecology in a changing environment: perspectives from the Quaternary. *Proc. Natl. Acad. Sci. U. S. A.* 112, 4915–4921
53. Allen, C.D. and Breshears, D.D. (1998) Drought-induced shift of a forest–woodland ecotone: rapid landscape response to climate variation. *Proc. Natl. Acad. Sci. U. S. A.* 95, 14839–14842
54. Williams, J.W. and Jackson, S.T. (2007) Novel climates, no-analog communities, and ecological surprises. *Front. Ecol. Environ.* 5, 475–482
55. Allen, C.D. (2016) Chapter 4. Forest ecosystem reorganization underway in the Southwestern US: A preview of widespread forest changes in the Anthropocene? In *Forest Conservation and Management in the Anthropocene: Adaptation of Science, Policy, and Practice* (Sample, V.A., Bixler, R.P. and Miller, C., eds), pp. 57–79, University Press of Colorado, 336 pp
56. Scheffer, M. *et al.* (2009) Early-warning signals for critical transitions. *Nature* 461, 53–59
57. Boettiger, C. and Hastings, A. (2013) Tipping points: from patterns to predictions. *Nature* 493, 157–158
58. Kriegler, E. *et al.* (2009) Imprecise probability assessment of tipping points in the climate system. *Proc. Natl. Acad. Sci. U. S. A.* 106, 5041–5046
59. Rogers, B.M. *et al.* (2015) Influence of tree species on continental differences in boreal fires and climate feedbacks. *Nat. Geosci.* 8, 228
60. Enquist, B.J., Michaletz, S.T. and Kerkhoff, A.J. (2016) Toward a general scaling theory for linking traits, stoichiometry, and body size to ecosystem function. In *A Biogeoscience Approach to Ecosystems* (Johnson, E.A. and Martin, Y., eds), Cambridge University Press
61. Hicke, J.A. *et al.* (2012) Effects of biotic disturbances on forest carbon cycling in the United States and Canada. *Glob. Change Biol.* 18, 7–34
62. McDowell, N. *et al.* (2010) Growth, carbon-isotope discrimination, and drought-associated mortality across a Pinus ponderosa elevational transect. *Glob. Change Biol.* 16, 399–415
63. Novick, K.A. *et al.* (2016) The increasing importance of atmospheric demand for ecosystem water and carbon fluxes. *Nat. Clim. Change* 6, 1023–1027
64. Zwiers, F.W. *et al.* (2013) Climate extremes: challenges in estimating and understanding recent changes in the frequency and intensity of extreme climate and weather events. In *Climate Science for Serving Society*, pp. 339–389, Netherlands, Springer
65. Bürger, G. *et al.* (2012) Downscaling extremes – an intercomparison of multiple statistical methods for present climate. *J. Clim.* 25, 4366–4388
66. Macias Fauria, M. *et al.* (2011) Predicting climate change effects on wildfires requires linking processes across scales. *Wiley Interdiscip. Rev. Clim. Change* 2, 99–112
67. Hantson, S. *et al.* (2016) The status and challenge of global fire modelling. *Biogeosciences* 13, 3359–3375
68. Bentz, B.J. *et al.* (2013) Climate change and bark beetles of the western United States and Canada: direct and indirect effects. *Bioscience* 60, 602–613
69. Chen, F. *et al.* (2015) An observational and modeling study of impacts of bark beetle-caused tree mortality on surface energy and hydrological cycles. *J. Hydrometeorol.* 16, 744–761
70. Mikkelson, K.M. *et al.* (2013) Bark beetle infestation impacts on nutrient cycling, water quality and interdependent hydrological effects. *Biogeochemistry* 115, 1–21
71. Guardiola-Claramonte, M. *et al.* (2011) Decreased streamflow in semi-arid basins following drought-induced tree die-off: a counter-intuitive and indirect climate impact on hydrology. *J. Hydrol.* 406, 225–233
72. Adams, H.D. *et al.* (2012) Ecohydrological consequences of drought-and infestation-triggered tree die-off: insights and hypotheses. *Ecohydrology* 5, 145–159
73. Biederman, J.A. *et al.* (2015) Recent tree die-off has little effect on streamflow in contrast to expected increases from historical studies. *Water Resour. Res.* 51, 9775–9789
74. Penn, C.A. *et al.* (2016) Numerical experiments to explain multiscale hydrological responses to mountain pine beetle tree mortality in a headwater watershed. *Water Resour. Res.* 52, 3143–3161
75. Nyman, P. *et al.* (2015) Predicting sediment delivery from debris flows after wildfire. *Geomorphology* 250, 173–186
76. Sidman, G. *et al.* (2016) Risk assessment of post-wildfire hydrological response in semiarid basins: the effects of varying rainfall representations in the KINEROS2/AGWA mode. *Int. J. Wildland Fire* 25, 268–278
77. Folke, C. *et al.* (2004) Regime shifts, resilience, and biodiversity in ecosystem management. *Annu. Rev. Ecol. Evol. Syst.* 35, 557–581
78. Michaletz, S.T. and Johnson, E.A. (2007) How forest fires kill trees: a review of the fundamental biophysical processes. *Scand. J. For. Res.* 22, 500–515
79. Woods, P. (1989) Effects of logging, drought, and fire on structure and composition of tropical forests in Sabah, Malaysia. *Biotropica* 21, 290–298

80. Breshears, D.D. *et al.* (2009) Tree die-off in response to global change-type drought: Mortality insights from a decade of plant water potential measurements. *Front. Ecol. Environ.* 7, 185–189
81. Michaletz, S.T. *et al.* (2014) Convergence of terrestrial plant production across global climate gradients. *Nature* 512, 39–43
82. Michaletz, S.T. and Johnson, E.A. (2008) A biophysical process model of tree mortality in surface fires. *Can. J. For. Res.* 38, 2013–2029
83. Bennett, A.C. *et al.* (2015) Larger trees suffer most during drought in forests worldwide. *Nat. Plants* 1, 15139
84. Michaletz, S.T. *et al.* (2012) Moving beyond the cambium necrosis hypothesis of post-fire tree mortality: cavitation and deformation of xylem in forest fires. *New Phytol.* 194, 254–263